Non-planar Dzyaloshinskii spirals in magnetic domains and domain walls in crystals with orthorhombic anisotropy

M. Heide,[1,2] G. Bihlmayer,[1] and S. Blügel[1]

[1]*Institut für Festkörperforschung & Institute for Advanced Simulation, Forschungszentrum Jülich, 52425 Jülich, Germany*

[2]*Department of Precision Science and Technology, Graduate School of Engineering, Osaka University, Suita, Osaka 565-0871, Japan*

(Dated: December 7, 2009)

The basic micromagnetic models of Landau, Lifshitz, and Dzyaloshinskii, have been extended by an anisotropy term with two independent parameters. The resulting ground states of the magnetic domains and the domain-wall profiles are discussed for crystal lattices with orthorhombic unit cells. In these simple geometries, the magnetization is not confined to a single plane. Depending on the relations between the spin-stiffness, anisotropy, and Dzyaloshinskii-Moriya interaction several different zero-temperature phases of the magnetic structure were found. The corresponding phase diagrams are obtained numerically. Analytical results are given for some special cases. The studied model is of particular relevance for magnetic wires, nanostripes and ultrathin magnetic films deposited on non-magnetic surfaces.

Keywords: domain wall, nanomagnetism, Dzyaloshinskii-Moriya, spin spiral

PACS numbers:

I. INTRODUCTION

In a classical model, magnetic moments can be considered as vector quantities, residing on atomic sites. In ferro- or antiferromagnets they are oriented parallel or antiparallel, respectively, depending on the exchange interaction. The moments point along an easy axis, relative to the crystal axis or the shape of the sample. Typically such a magnet is not in a single domain state, but splits up into a multidomain state, where domains are separated by domain walls. The mesoscale structures and the properties of the domains and domain walls play a crucial role in magnetism as the domain-wall nucleation, propagation and annihilation are the driving mechanisms in magnetization reversal in response to an external magnetic field.

Textbook examples of such mesoscale structures are ferromagnetic domains separated by Bloch or Néel walls. Within in a Bloch wall, the magnetization rotates like a helical spiral in the plane parallel to the wall normal, while within the Néel wall the magnetization rotates like a cycloidal spiral in a plane perpendicular to the wall normal. Already in 1932 Bloch[1] pointed out that the wall structure is determined by the competition between the exchange and anisotropy energies and the exact internal structure of the Bloch wall has been calculated first by Landau and Lifshitz.[2] Néel[3] has shown that an additional dipolar interaction can lead to a new type of wall, carrying his name. In fact in realistic systems there are further effects that may become important. For example in sufficiently thick magnetic samples, the influence of the long-ranged magnetostatic interactions can lead to a variety of complex domain-wall structures (cf. Ref. 4).

In recent years the investigation of the magnetic structure in nanomagnets moved into the focus of intensive research. This interest is in part motivated by the prospect of using nanomagnets in novel magnetic memory or logic devices[5–9]. Their construction requires a profound understanding of the magnetic structure, energy and properties of domains and walls. Interest is also stimulated by new experimental techniques such as the spin-polarized scanning tunneling microscope (SP-STM) and magnetic force microscopy (MFM) which provide new insight to the magnetic structure in on the atomic scale[10–13].

Compared to bulk systems, in nanomagnets several factors may alter the energetics or the magnetic structure. The long-ranged nature of the magnetostatic interactions plays a crucial role in the formation of most of the studied domain patterns. In low-dimensional or very small samples, however, it is of minor importance. Also the material parameters that determine the short-ranged interactions change, if the spatial dimensions are reduced by surfaces and interfaces.[14–17] This paper addresses an aspect typical for nanomagnets, that attracted a lot of attention in the last years: For a magnetic system the lack of space inversion symmetry together with the presence of the spin-orbit interaction gives rise to the Dzyaloshinskii-Moriya (DM) interaction[18,19]. This interaction is antisymmetric with respect to the rotational direction, i.e. it favors spatially rotating magnetic structures of a certain handedness. This interaction can always be expected at surfaces[20], and resulting spatially rotating magnetic structures have recently been observed in ultrathin films[21,22] and proposed for other low-dimensional systems (cf. e.g. Refs. 23**?** –25). Even in cases where the DM interaction is not strong enough to induce a rotating ground state, it have a significant influence on the energetics of the domain walls and thus influence the entire domain structure.[26]

Dzyaloshinskii[27] was the first to study the consequence

of this interaction for the mesoscale magnetic structure. He applied a micromagnetic model in which the magnetization can vary along one spatial direction, x, and is described by a single angle $\varphi(x)$. He showed that the DM interaction may generate periodically modulated magnetic structures. There are many possible ways to extend Dzyaloshinskii's basic model by including higher-order exchange or anisotropy terms. If one considers more than one spatial dimension and allows for certain higher-order interactions or an external magnetic field, the model can support more complex structures like vortices and skyrmions, and the understanding of these magnetic structures increased significantly in recent years.[28–32]

In this paper we do not allow for higher-order terms or more than one spatial dimension, but extend the micromagnetic model by allowing for two independent anisotropy terms as they appear in orthorhombic crystal structures or rectangular unit cells at a surface. The resulting micromagnetic ground state is investigated theoretically. Thereby, we find a variety of distinct magnetic phases and discuss the occurrence of these phases with respect to the values of the spin stiffness, magnetic anisotropy and DM interaction. For certain choices of the model parameters the ground-state magnetization is not confined to a plane but varies on a truly three-dimensional path in spin space. Besides the ground state in the domains, we discuss the domain walls. They can be strongly altered by the interplay of DM interaction and magnetocrystalline anisotropy, even if the domain magnetization is collinear.

Our model aims at ultrathin magnetic films and chains deposited on non-magnetic substrates, but holds also for other nanostructures and bulk crystals which lack centrosymmetry and for which the long-ranged nature of the magnetostatic interaction can be neglected (e.g. antiferromagnets). The equations are worked out in detail for orthorhombic unit cells, which include for example (110) oriented thin films or surfaces of cubic crystals and clusters deposited on appropriate substrates.

In section II we introduce the studied micromagnetic model and briefly discuss its applicability. In section III the possible magnetic structures of this model are investigated numerically. The dependence of the magnetic structure on the model parameters is investigated and the resulting phase diagrams are presented. For some cases there are simple analytical solutions, these are presented in section IV.

II. MODEL

We restrict our analysis to a simple micromagnetic model, i.e. we describe the magnetization in terms of a continuum theory. The magnetization direction is described by a continuous normalized function $\mathbf{m}(x)$ that varies only along one spatial coordinate x over length scales significantly larger than the crystal lattice constant. If we want to describe locally antiferromagnetic structures, we assume that the atoms' magnetic moments are aligned alternately parallel and antiparallel to $\mathbf{m}$.

In the studied model, the energy is approximated by the functional

$$E[\mathbf{m}] = \int \mathrm{d}x \Big[A \Big(\frac{\mathrm{d}\,\mathbf{m}}{\mathrm{d}\,x} \Big)^2 + \mathbf{D} \cdot \Big(\mathbf{m} \times \frac{\mathrm{d}\,\mathbf{m}}{\mathrm{d}\,x} \Big) + \mathcal{K}\big(\mathbf{m}\big) \Big] \quad (1)$$

with $|\mathbf{m}(x)| = 1$. The integrand is a one-dimensional energy density. It is a local function of $\mathbf{m}$ and $\mathrm{d}\,\mathbf{m}/\mathrm{d}\,x$. It contains the leading symmetric and antisymmetric terms in $\mathrm{d}\mathbf{m}/\mathrm{d}x$ as well as an anisotropy term. The first term accounts for the spin stiffness A. It is dominated by non-relativistic exchange interactions. The second term represents the DM interaction with the Dzyaloshinskii vector $\mathbf{D}$. It is of purely relativistic origin (i.e. due to spin-orbit coupling). The last term, $\mathcal{K}$, is a function that depends only on $\mathbf{m}$. It describes the anisotropy of the system and is due to the spin-orbit coupling and to magnetostatic interactions. The first term favors a collinear spin alignment (i.e. $\mathbf{m}(x) = \text{const}$), it is isotropic in spin space and symmetric with respect to the direction of the spin rotations (i.e. with respect to $\mathrm{sign}(\mathrm{d}\mathbf{m}/\mathrm{d}x)$). The third term favors a certain magnetization direction and thus also supports a collinear spin alignment. The second term, however, favors non-collinear structures with $\mathbf{m}$ spatially rotating in the plane normal to the $\mathbf{D}$-vector. Thus, it competes both with the first and the third term. The DM interaction does not influence the energy of spin rotations in a plane parallel to $\mathbf{D}$, but for rotations in the plane normal to $\mathbf{D}$ it distinguishes between the two rotational directions.

A. Assumptions and applicability

First, we discuss the main assumptions that enter our ansatz (1):

The restriction to one spatial coordinate x a priori excludes more-dimensional magnetic structures like the recently discussed vortex or skyrmion type magnetic structures.[28,31,32] This does not present a problem if we want to describe magnetic chains or nanostripes, or materials with a sufficiently anisotropic spin stiffness, and the assumption is expected to be reasonable for the discussion of simple domain walls between ferromagnetic domains. In Ref. 29 the functional (1) is generalized to two spatial coordinates in order to describe extended films, but restricted to uniaxial anisotropy. For that case it is shown that the ground-state magnetization in absence of a magnetic field varies only along one spatial direction. It remains to be investigated if this result still holds for systems where $A, \mathbf{D}, \mathcal{K}$ are anisotropic with respect to the spatial coordinates.

The applicability of a continuous model implies that $\mathbf{m}(x)$ varies on length scales that are large compared to the lattice spacing. As the energy density is a local function of $\mathbf{m}$ and $\mathrm{d}\mathbf{m}/\mathrm{d}x$, we assume that $\mathbf{m}(x)$

is sufficiently constant over the range of the dominating magnetic interactions. This assumption might not hold, if the magnetic structure is influenced either by long-ranged RKKY interactions or by long-ranged magnetostatic (dipole-dipole) interactions. The former interaction plays and significant role in diluted magnetic systems, the latter one plays an important role in bulk material and thick magnetic films. In the case of atomically thin films and other magnetic nanostructures, however, the corresponding magnetic fields are relatively weak and only the dipole-dipole interactions between neighboring atoms can have a significant influence on the local magnetic structure. This influence can be modeled with the local anisotropy term $\mathcal{K}(\mathbf{m})$.[33] In typical magnets the non-relativistic exchange interactions are the largest energy contributions to Eq. (1) and determine the magnetic structure on the atomic scale. If they favor a collinear magnetic phase (with $\mathbf{m}(x) = \text{const}$), we expect them to be strong enough to prevent any short-ranged modulations of the magnetic structure. In this case, we can work with the leading terms in $\mathbf{m}$ and $\mathrm{d}\mathbf{m}/\mathrm{d}x$ and summarize all symmetric and antisymmetric exchange interactions in the spin stiffness A and the Dzyaloshinskii vector $\mathbf{D}$.

The model should be useful for the description of atomically thin magnetic films, stripes, and wires deposited on non-magnetic substrates: Besides the possibility to approximate the magnetostatic dipole-dipole interaction by the local anisotropy term, all magnetic atoms in these systems are exposed to a strongly inversion-asymmetric environment. Thus one can expect a relatively large DM interaction, in which case our study can become relevant.

B. Model parameters

In this paper, we neglect external magnetic fields, and we restrict our investigations to crystal structures with mutually orthogonal lattice vectors and an anisotropy term that can be approximated by the diagonal tensor K:

$$\mathcal{K}(\mathbf{m}) = \mathbf{m}^\dagger \cdot \mathsf{K} \cdot \mathbf{m} \quad \text{with} \quad \mathsf{K} = \begin{pmatrix} K_1 & 0 & 0 \\ 0 & K_2 & 0 \\ 0 & 0 & K_D \end{pmatrix} \tag{2}$$

whereby $\mathbf{m}$ is represented in a Cartesian coordinate system.

In many cases, the direction of the $\mathbf{D}$-vector can be deduced directly from symmetry. For example if the x-direction of varying magnetization $\mathbf{m}(x)$ lies in a mirror plane of the crystal, the we have to consider a Dzyaloshinskii vector normal to this mirror plane. In the following, we assume that the Dzyaloshinskii vector $\mathbf{D}$ points along a high-symmetry line of the crystal and choose

$$\mathbf{D} = D\,\hat{\mathbf{e}}_3 \,. \tag{3}$$

(In ultrathin films, $\mathbf{D}$ typically is parallel to the film plane. In such cases $\hat{\mathbf{e}}_3$ is orthogonal to the usually chosen z-axis.)

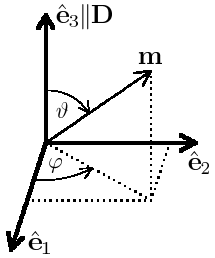

FIG. 1: Orientation of the Cartesian coordinate system and definition of the polar angles ϑ, φ. $\hat{\mathbf{e}}_3$ is chosen parallel to the $\mathbf{D}$-vector.

In the following, we describe the magnetization $\mathbf{m}$ with the (x-dependent) polar angles ϑ and φ (cf. Fig. 1):

$$\mathbf{m} = \sin\vartheta\,\cos\varphi\,\hat{\mathbf{e}}_1 + \sin\vartheta\,\sin\varphi\,\hat{\mathbf{e}}_2 + \cos\vartheta\,\hat{\mathbf{e}}_3 \,. \tag{4}$$

The model as given by Eqs. (1-2) can be described with two reduced parameters instead of A, D, and K. Introducing

$$D_\mathrm{I} = \frac{D}{\sqrt{A\,(K_2 - K_1)}} \quad , \quad K_\mathrm{I} = \frac{K_D - K_1}{K_2 - K_1} \,, \tag{5}$$

we can simplify the following calculations by scaling the length and energy by

$$x_\mathrm{I} = \frac{x}{\sqrt{A/(K_2 - K_1)}} \quad , \quad E_\mathrm{I} = \frac{E}{\sqrt{A\,(K_2 - K_1)}} \,, \tag{6}$$

i.e. we express x and E in terms of the width $2\sqrt{A/K}$ and energy $4\sqrt{A\,K}$ of a domain wall that is confined to a plane parallel to $\hat{\mathbf{e}}_3$ (cf. Ref. 2). Inserting Eqs. (4-6) in the energy functional (1) yields

$$E_\mathrm{I} = \int \mathrm{d}x_\mathrm{I} \Big[\dot{\vartheta}^2 + \sin^2\vartheta \left(\dot{\varphi}^2 + D_\mathrm{I}\,\dot{\varphi} + \sin^2\varphi - K_\mathrm{I} \right) + \text{const} \Big] \,. \tag{7}$$

Hereby, we used the notations

$$\vartheta = \vartheta(x_\mathrm{I}) \,,\ \varphi = \varphi(x_\mathrm{I}) \,,\ \dot{\vartheta} = \tfrac{\mathrm{d}}{\mathrm{d}x_\mathrm{I}}\,\vartheta(x_\mathrm{I}) \,,\ \dot{\varphi} = \tfrac{\mathrm{d}}{\mathrm{d}x_\mathrm{I}}\,\varphi(x_\mathrm{I}) \,.$$

In order to access the case $K_2 \leq K_1$ as well, we introduce as a second set of reduced parameters

$$D_\mathrm{II} = \frac{D}{\sqrt{A\,(K_2 - K_D)}} \quad , \quad K_\mathrm{II} = \frac{K_1 - K_D}{K_2 - K_D} \,, \tag{8}$$

and the appendant scaled length and energy

$$x_\mathrm{II} = \frac{x}{\sqrt{A/(K_2 - K_D)}} \quad , \quad E_\mathrm{II} = \frac{E}{\sqrt{A\,(K_2 - K_D)}} \,. \tag{9}$$

For vanishing D, the last denominators correspond to the width and energy of a wall that is confined to the plane normal to $\hat{\mathbf{e}}_3$. Inserting (8-9) in (1) yields

$$E_\mathrm{II} = \int \mathrm{d}x_\mathrm{II} \Big[\dot{\vartheta}^2 + \sin^2\vartheta \left(\dot{\varphi}^2 + D_\mathrm{II}\,\dot{\varphi} + \sin^2\varphi + K_\mathrm{II}\,\cos^2\varphi \right) + \text{const} \Big] \,, \tag{10}$$

where we used the notations

$$\vartheta = \vartheta(x_{\text{II}})\,,\ \varphi = \varphi(x_{\text{II}})\,,\ \dot{\vartheta} = \tfrac{\mathrm{d}}{\mathrm{d}x_{\text{II}}}\,\vartheta(x_{\text{II}})\,,\ \dot{\varphi} = \tfrac{\mathrm{d}}{\mathrm{d}x_{\text{II}}}\,\varphi(x_{\text{II}})\,.$$

In the following, we switch between $(D_{\text{I}}, K_{\text{I}})$ and $(D_{\text{II}}, K_{\text{II}})$ in order to keep the formulas simple.

The magnetic ground state is given by the functions $\vartheta(x)$ and $\varphi(x)$ that minimize E_{I} and E_{II} respectively. In order to study domain walls, we introduce boundary conditions for $x \to \pm\infty$. If the domains are homogeneously collinear magnetized, a wall between two oppositely magnetized domains is determined by the minimal solution of Eq. (7) or Eq. (10) under the boundary condition

$$\mathbf{m}(x) \overset{x\to\pm\infty}{\longrightarrow} \pm\mathbf{m}_{\text{easy}}\ , \tag{11}$$

where $\mathbf{m}_{\text{easy}}$ denotes the magnetization direction parallel to the easy axis.

III. MAGNETIZATION SHAPES AND PHASE TRANSITIONS

In this section we discuss the solutions that minimize the energy functionals (7,10). If the Dzyaloshinskii vector points parallel to the hard axis (i.e. $K_1, K_2 < K_D$), then all terms in the functional (1) favor a magnetization that stays in the plane normal to $\mathbf{D}$ (i.e. $\vartheta = \pi/2$, $\dot{\vartheta} = 0$). In this case, $\mathbf{m}(x)$ can be described by a single angle φ and the corresponding magnetic structures are elaborately discussed in literature.[27,34]

A. Magnetic ground state in the domains

In the next paragraphs we seek the ground state of (7,10) without any constraints or boundary conditions for $|x| \to \infty$, thus we are not requesting a particular domain structure.

At first, we assume that the Dzyaloshinskii vector points parallel to the hard axis. As mentioned above, this implies $\vartheta \equiv \pi/2$. Without loss of generality, we can assume that $K_1 \le K_2 < K_D$ and Eq. (7) yields (after neglecting any constant term in the integrand):

$$E_{\text{I}}\Big|_{\vartheta\equiv\frac{\pi}{2}} = \int \mathrm{d}x_{\text{I}}\left(\dot{\varphi}^2 + D_{\text{I}}\,\dot{\varphi} + \sin^2\varphi\right)\ . \tag{12}$$

The ground state of Eq. (12) is already discussed by Dzyaloshinskii, we will briefly state his results. For further details and analytical derivations confer Refs. 27,34. If we neglect the anisotropy term $\sin^2\varphi$, we obtain spin rotations for all non-vanishing D_{I}. But, for small D_{I} the DM term cannot compete with the sum $\dot{\varphi}^2 + \sin^2\varphi$ and the energy is minimized by a collinear magnetization that is oriented along the easy axis (i.e. $\varphi(x) \equiv 0$). The model (12) shows a spatially rotating magnetization as the ground state, if and only if

$$|D_{\text{I}}| > \frac{4}{\pi}\ . \tag{13}$$

In the following, we denote the period length of a spatially rotating ground state with λ. In the case of model (12), λ diverges for $|D_{\text{I}}| \searrow \frac{4}{\pi}$. This transition can be interpreted as a second-order phase transition with order parameter $1/\lambda$ and a kink in $\mathrm{d}E_{\text{I}}/\mathrm{d}D_{\text{I}}$. If the magnetization rotates, then the sign of $\dot{\varphi}$ is opposite to the sign of D_{I}.

Next, we discuss the case that the Dzyaloshinskii vector does not point parallel to the hard axis. We assume $K_D < K_2$ and $K_1 \le K_2$ ($\Rightarrow K_{\text{II}} \le 1$). In this case, the angle ϑ is determined by a competition between the DM and the anisotropy terms: The energy gain from $\sin^2\vartheta\, D_{\text{II}}\,\dot{\varphi}$ is maximal for $\vartheta = \pi/2$, but in this case a full rotation ($\varphi{=}0 \to \varphi{=}\pm2\pi$) does not avoid $\mathbf{m}$ parallel to the hard axis. In the most simple case, $\mathbf{D}$ points parallel to the easy axis the anisotropy in the plane normal to the Dzyaloshinskii vector can be neglected ($K_1 = K_2 > K_D$, $K_{\text{II}} = 1$). Then Eq. (10) simplifies to

$$E_{\text{II}}\Big|_{K_{\text{II}}=1} = \int \mathrm{d}x_{\text{II}}\left[\dot{\vartheta}^2 + \sin^2\vartheta\left(\dot{\varphi}^2 + D_{\text{II}}\,\dot{\varphi} + 1\right)\right]\ . \tag{14}$$

Obviously, this functional is isotropic in φ and minimized by $\dot{\varphi} = \text{const}$, $\vartheta = \text{const}$. If $|D_{\text{II}}|$ is small, then the term $(\dot{\varphi}^2 + D_{\text{II}}\,\dot{\varphi} + 1)$ is positive for all $\dot{\varphi}$ and (14) is minimal for the collinear solution $\sin^2\vartheta \equiv 0$. If $|D_{\text{II}}|$ is sufficiently large (i.e. $|D_{\text{II}}| > 2$, cf. section IV A), then the DM term can compete with the spin stiffness and anisotropy terms (i.e. $\dot{\varphi}^2 + D_{\text{II}}\,\dot{\varphi} + 1 < 0$) and (14) is minimal for $\sin^2\vartheta \equiv 1$. Thus, for increasing $|D_{\text{II}}|$ the system undergoes a first-order transition from the collinear state to a flat noncollinear state that is spatially rotating in the plane normal to the easy axis.

The situation is less concise, if the plane normal to the Dzyaloshinskii vector is not isotropic. In this case, the competition between the DM and the anisotropy term can result in another rotating phase where the angle ϑ is not constant but depends on φ. Then, the ground-state magnetization $\mathbf{m}(x)$ describes a truly three-dimensional path in spin space (cf. Fig. 2). We investigated Eq. (10) numerically in order to locate the different magnetic ground states in the $(D_{\text{II}}, K_{\text{II}})$-space. The resulting phase diagram is shown in Fig. 3. In this diagram, the region of the three-dimensional magnetization is bounded by two critical lines where $\mathbf{m}$ undergoes second-order phase transitions (i.e., if a path in the $(D_{\text{II}}, K_{\text{II}})$-space is defined by the smooth functions $D_{\text{II}}(p)$ and $K_{\text{II}}(p)$ then $\mathrm{d}\,E_{\text{II}}/\mathrm{d}\,p$ is continuous but not smooth at a critical line). Thus, if $\mathbf{D}$ points parallel to the easy axis ($0 < K_{\text{II}} \neq 1$) then the magnetization can vary continuously from a collinear state parallel to the easy axis to a flat rotating state. Note, that in this case the spatial period length does not diverge in the vicinity of the collinear ground state. A continuous transition from a collinear state to a rotating state of finite period length is possible only if $\mathbf{D}$ points parallel to the easy axis, since the rotating structures gain energy from the rotation around the Dzyaloshinskii vector (cf. section IV A). In section IV A it is shown, that the critical line that is bordering the

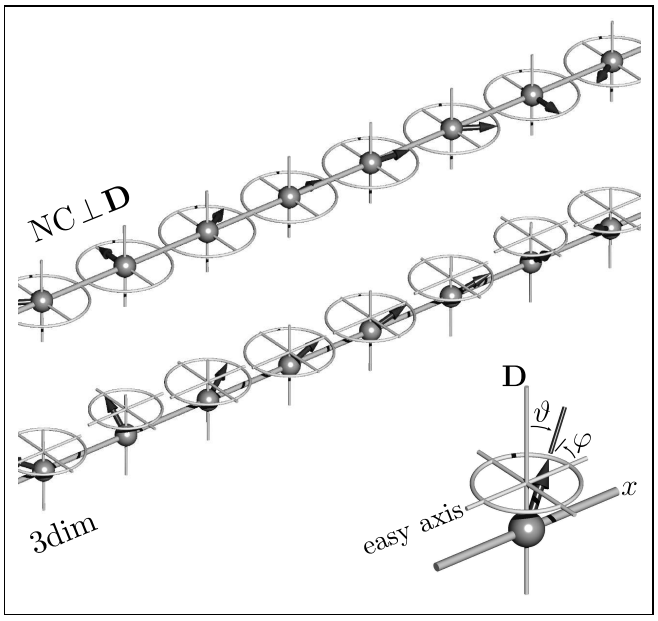

FIG. 2: Noncollinear magnetization in the domains. The arrows represent the magnetization $\mathbf{m}$ that is defined by $\vartheta(x)$ and $\varphi(x)$. In the top image (NC $\perp$ **D**) the magnetization is confined to the plane normal to **D**, whereas in the bottom image (3dim) it describes a truly three-dimensional path in spin space. In this case there is $\vartheta \neq$ const, since $\mathbf{m}$ tries to avoid the hard axis. The images are calculated with $K_{\rm II} = -0.04$, and $D_{\rm II} = 1.38$ (NC$\perp$**D**) and $D_{\rm II} = 1.30$ (3dim) respectively.

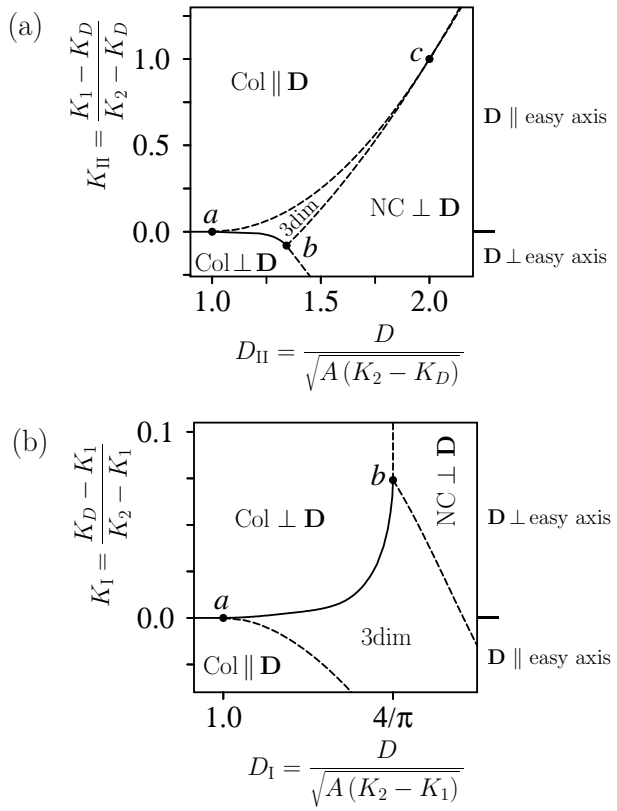

FIG. 3: Phase diagram of the domain magnetization. For $D > 0$, the diagram shows four distinct phases, namely the collinear phases with $\mathbf{m}$ pointing parallel to the easy axis and parallel or perpendicular to the Dzyaloshinskii vector (Col $\parallel$ **D** or Col $\perp$ **D**), the noncollinear phase with $\vartheta(x) = \frac{\pi}{2} =$ const (NC $\perp$ **D**), and the noncollinear phase with $\mathbf{m}(x)$ describing a truly three-dimensional path in spin space (3dim). The solid lines denote first-order and the dashed lines second-order transitions. At point c ($D_{\rm II} = 0$, $K_{\rm II} = 1$) the dashed lines touch, at this point the system shows a sharp transition from Col $\parallel$ **D** to NC $\perp$ **D**. $D_{\rm I}$ and $K_{\rm I}$ diverge at point c, whereas a ($D_{\rm I} = 1$, $K_{\rm I} = 0$) and b ($D_{\rm I} = \frac{4}{\pi}$) correspond to the same sets of parameters A, D, K both in Figs. (a) and (b).

collinear state (line a-c in Fig. 3a) is defined by

$$K_{\rm II} = D_{\rm II}^2 - 2\,|D_{\rm II}| + 1 \quad \text{for} \quad |D_{\rm II}| > 1 \qquad (15)$$

or, equivalently,

$$K_{\rm I} = -\frac{D_{\rm I}^4 - 2\,D_{\rm I}^2 + 1}{4\,D_{\rm I}^2} \quad \text{for} \quad |D_{\rm I}| > 1\,. \qquad (16)$$

Not shown in Fig. 3 are the equivalent phases of opposite chirality, that we obtain for $D < 0$ (remember, that $\operatorname{sign}\dot\varphi = -\operatorname{sign} D$). By our choice of reduced parameters (Eqs. (5-8)) we cannot describe the collinear phase with $\mathbf{m} = \hat{\mathbf{e}}_2$, but this phase is equivalent to the collinear phase with $\mathbf{m} = \hat{\mathbf{e}}_1$.

Before turning our attention to the domain walls, we note that oppositely magnetized domains can exist in the regimes of collinear or truly three-dimensional domain magnetizations. In the latter case, $\operatorname{sign} m_3$ is constant for the entire domain since in that regime $\vartheta \neq \pi/2$ (cf. Fig. 2). Therefore, in one domain $0 \leq \vartheta < \pi/2$, while in the other domain $\pi/2 < \vartheta \leq \pi$. In the regime of flat rotations, the possible magnetic structures differ only by a phase shift.

B. Domain walls

In this section we discuss the the domain-wall shapes and energies. For vanishing D the magnetization $\mathbf{m}(x)$ in the domain wall describes a path that minimizes the anisotropy energy, thus $\mathbf{m}(x)$ is confined to the plane perpendicular to the hard axis. In this case we can assume $K_1 < K_2 < K_D$ and work with the functional and boundary conditions

$$E_{\rm I} = \int \mathrm{d}x_{\rm I}\,\left(\dot\varphi^2 + \sin^2\varphi\right) \quad , \quad \varphi \overset{x_{\rm I}\to\pm\infty}{\longrightarrow} \frac{\pi}{2} \pm \frac{\pi}{2}\,. \qquad (17)$$

This model has the well known solution[2]

$$\varphi(x_{\rm I}) = \pm \arccos\tanh(-x_{\rm I})\,. \qquad (18)$$

If the Dzyaloshinskii vector is nonvanishing and parallel to the hard axis (i.e. if $K_{\rm I} > 1$), we employ Eq. (12). With the boundary conditions as stated in Eq. (17), we obtain $\int \mathrm{d}x_{\rm I}\,\dot\varphi = (\operatorname{sign}\dot\varphi)\,\pi$ and the energy functional sim-

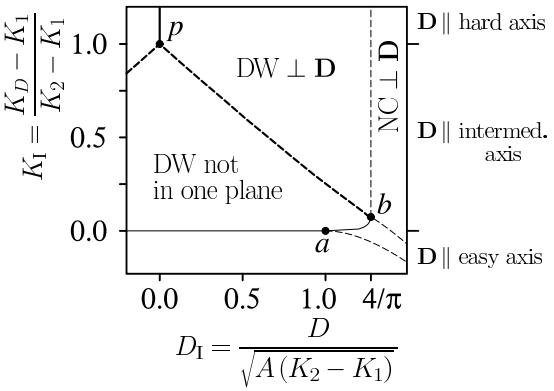

FIG. 4: Phase diagram of the domain walls. The thin lines separate the different phases of the domain magnetization, they are already described in Fig. 3b. The bold lines indicate the additional phase transitions of the domain walls. For large $K_{\rm I}$ the magnetization is confined to the plane normal to the Dzyaloshinskii vector (DW $\perp$ **D**). The solid line starting at p ($D_{\rm I} = 0, K_{\rm I} = 1$) indicates a first-order transition where the rotational direction changes (since $\operatorname{sign}\dot\varphi = -\operatorname{sign} D_{\rm I}$). The dashed line from p to b indicates the continuous transition from the flat to the truly three-dimensional domain walls (cf. Fig. 5). For $K_{\rm I} < 0$, the collinear domains are oriented parallel to **D** and we can obtain domain walls as illustrated in Fig. 6. In the regime with $\vartheta(x) = \frac{\pi}{2} = \text{const}$ (NC$\perp$ **D**) there are no domains of distinct magnetization directions.

plifies to

$$E_{\rm I} = \int \mathrm{d}x_{\rm I}\,\left(\dot\varphi^2 + \sin^2\varphi\right) \pm \pi\, D_{\rm I}\,. \qquad (19)$$

Thus, for **D** parallel to the hard axis, the optimal domain-wall shape does not depend on $|D_{\rm I}|$ and is still given by Eq. (18). Only the sign of the right-hand side of (18) depends on the sign of $D_{\rm I}$.

If the Dzyaloshinskii vector does not point parallel to the hard axis (i.e. if $K_{\rm I} < 1$), we work with Eqs. (7) and (10) again. In the regime of a three-dimensional domain magnetization, we have to replace the boundary conditions (11) by

$$x \gg 1 \;\Rightarrow\; \begin{cases} 0 < \vartheta(+x) < \frac{\pi}{2} \\ \frac{\pi}{2} < \vartheta(-x) < \pi \end{cases}\,. \qquad (20)$$

But even if the individual domains are collinear, the competition of the DM and the anisotropy term can result in a truly three-dimensional domain wall structure. If the Dzyaloshinskii vector points parallel to the intermediate axis (i.e. $0 < K_{\rm I} < 1$), we find a continuous transition from a wall that is confined to the plane normal to the hard axis (at vanishing D) to a wall that is confined to the plane normal to the **D**-vector (as favored by the DM term). Only for $D = 0$ the domain-wall magnetization is exactly perpendicular to the hard axis, but for all $|D|$ beyond a certain critical value it is exactly perpendicular to the Dzyaloshinskii vector. The resulting phase diagram

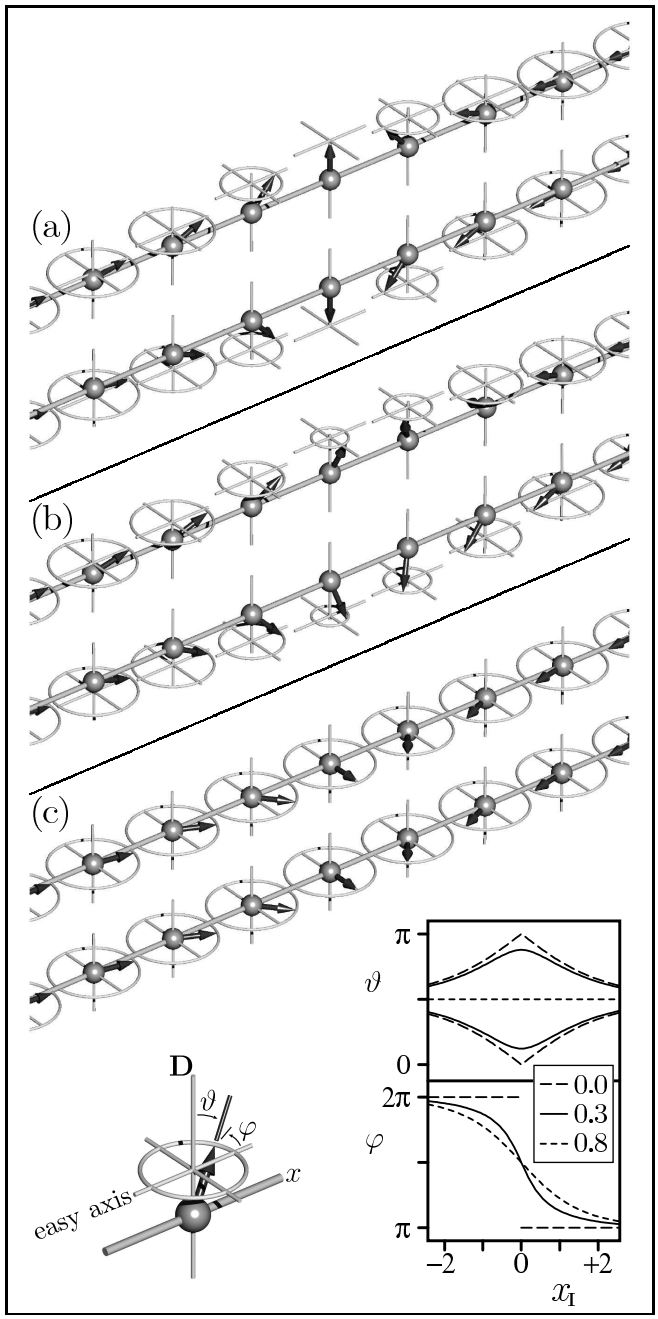

FIG. 5: Rotation paths of $\mathbf{m}(x)$ in the walls between collinear domains, the **D**-vector is perpendicular to the easy axis (i.e. $K_{\rm I} > 0$). The inset shows the polar angles for $K_{\rm I} = 0.5$ and $D_{\rm I}$ as specified in the legend. (a): For $D_{\rm I} = 0$ and $0 < K_{\rm I} < 1$ there are two degenerate rotation paths in the plane normal to the hard axis (cf. inset, $D_{\rm I} = 0$). (b): For small $D_{\rm I} > 0$ and $0 < K_{\rm I} < 1$ the competition between the anisotropy term and the DM term results in a three-dimensional rotation path in spin space. There are still two degenerate solutions (cf. inset, $D_{\rm I} = 0.3$). (c): For larger $D_{\rm I}$ or $K_{\rm I} > 1$ the magnetization is confined to the plane normal to **D**. In this case, there is only one solution: the continuations of both configurations in (b) coincide in the regime of $\mathbf{m} \perp \mathbf{D}$ (cf. inset, $D_{\rm I} = 0.8$).

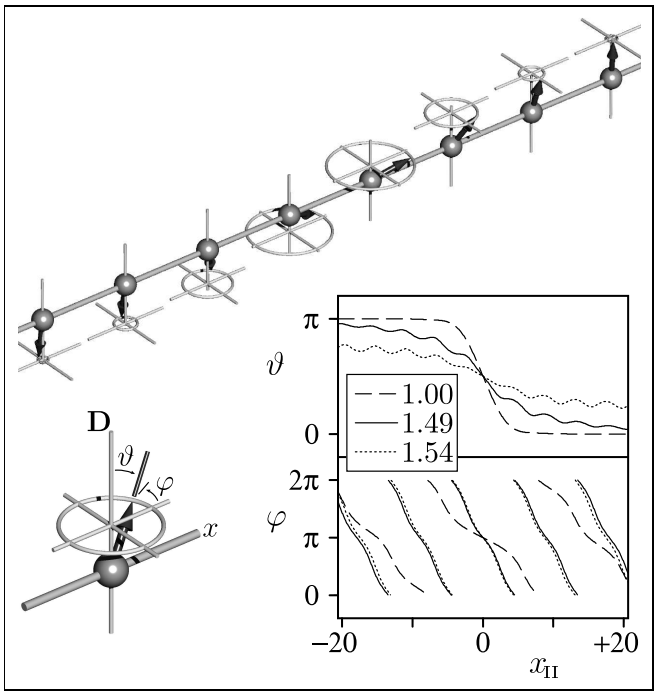

FIG. 6: Rotation path of $\mathbf{m}(x)$ in the walls between collinear domains, the $\mathbf{D}$-vector is parallel to the easy axis (i.e. $K_{\rm I} < 0$). For $K_{\rm II} = 1$ the magnetization describes a homogeneous rotation ($\dot\varphi = \text{const}$) around the Dzyaloshinskii vector. The inset shows more complex structures that arise if the plane normal to $\mathbf{D}$ is not isotropic, these polar angles are calculated with $K_{\rm II} = 0.25$ and $D_{\rm II}$ as specified in the legend. Note, that the transition from collinear to three-dimensional domain magnetization occurs at $D_{\rm II} = 1 + \sqrt{K_{\rm II}} = 1.5$. Not shown are the degenerate solutions with φ shifted by π.

is given in Fig. 4. For vanishing D there are two energetically degenerate solutions of opposite rotational direction. The corresponding rotation axis is the hard axis. For $\mathbf{D}$ perpendicular to the hard axis ($K_{\rm I} < 1$), this degeneracy is not lifted in the regime of three-dimensional wall structures. For increasing $|D|$ the two degenerate magnetization paths deform continuously and coincide at the critical line (line p-b in Fig. 4). The magnetic structures are illustrated in Fig. 5. If the Dzyaloshinskii vector points parallel to the easy axis (i.e. $K_{\rm I} < 0$, $K_{\rm II} > 0$), the magnetization path can show more than a half rotation around the Dzyaloshinskii vector: φ decreases steadily while ϑ asymptotically converges to 0. Such magnetic structures are illustrated in Fig. 6.

In Fig. 7 we show the influence of the DM term on the wall energies. Thereby, we choose the constant terms in the integrands of Eqs. (7,10) such that the domain magnetization does not contribute to the energy. If the magnetization is confined to the plane normal to the $\mathbf{D}$-vector, we can insert the expression (18) in Eq. (19) and obtain[2]

$$E_{\rm I} = 4 - \pi\,|D_{\rm I}| \quad\Leftrightarrow\quad E = 4\,\sqrt{A\,(K_2 - K_1)} - \pi\,|D|\,. \quad (21)$$

If the magnetization is confined to a plane that includes

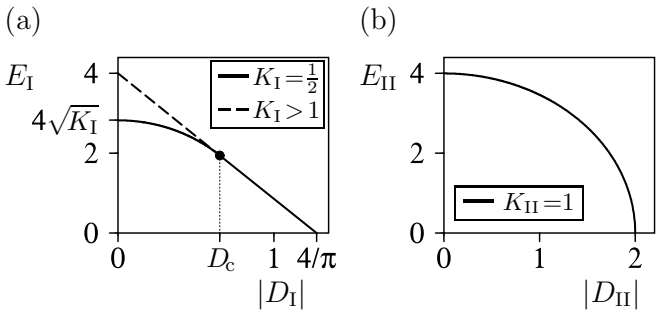

FIG. 7: Domain wall energies. Fig. a: The thick solid line represents the domain wall energies for fixed $K_{\rm I} = 0.5$. $D_{\rm c}$ denotes $D_{\rm I}$ on the critical line (line p-b in Fig. 4). For $D_{\rm c} < |D_{\rm I}| < \frac{4}{\pi}$ the magnetization is confined to the plane normal to the Dzyaloshinskii vector and the wall energy is given by $4 - \pi\,|D_{\rm I}|$. For $|D_{\rm I}| < D_{\rm c}$ the wall can reduce energy by deviating from the plane normal to the Dzyaloshinskii vector and for decreasing $|D_{\rm I}|$ the magnetic structure continuously transforms into a wall that is confined to the plane normal to the hard axis and has the energy $4\,\sqrt{K_{\rm I}}$. The dashed line indicates the wall energy for $K_{\rm I} > 1$, i.e. for $\mathbf{D}$ parallel to the hard axis. Fig. b: The curve shows the domain wall energy for the Dzyaloshinskii vector parallel to the easy axis. Thereby, we assume no anisotropy in the plane normal to $\mathbf{D}$.

$\mathbf{D}$, we obtain (for $\mathbf{m} \perp \hat{\mathbf{e}}_2$ and $K_D > K_1$)

$$E_{\rm I} = 4\,\sqrt{K_{\rm I}} \quad\Leftrightarrow\quad E = 4\,\sqrt{A\,(K_D - K_1)}\,. \quad (22)$$

Eq. (21) is consistent with the condition (13), as it implies a noncollinear domain magnetization for $|D_{\rm I}| > 4/\pi$.

C. Remarks concerning the numerical procedure

When minimizing the energy functionals (7,10), the magnetization $\mathbf{m}(x)$ is calculated on a real-space grid. In order to investigate the noncollinear domain magnetization, we employ periodic boundary conditions. We have to determine the optimal period length λ (i.e. λ with minimal energy density $E_{\rm II}/\lambda$) for each point in the $(D_{\rm II}, K_{\rm II})$-space. For each $K_{\rm II}$-value, we start at large $D_{\rm II}$ with the analytically known λ of the flat spirals and follow the local optimum of λ when decreasing $D_{\rm II}$ in small steps. This procedure reveals the existence of a three-dimensional structure that has lower energy than the collinear structures and flat spirals. But we cannot rule out more complex three-dimensional structures of even lower energy, that do not match with our choice of periodic boundary conditions.

The second-order phase transitions are detected by identifying the kinks in the $\frac{\rm d}{{\rm d}\,D_{\rm I}}\,E_{\rm I}(D_{\rm I})$-curves at fixed $K_{\rm I}$ and in the $\frac{\rm d}{{\rm d}\,D_{\rm II}}\,E_{\rm II}(D_{\rm II})$-curves at fixed $K_{\rm II}$, respectively. The derivatives are calculated from the difference quotients after minimizing the energy on a dense D-grid.

A detailed description of the numerical procedure is given in Ref. 35.

IV. ANALYTICALLY SOLVABLE CASES

For the case that the magnetization is confined to the plane normal to the Dzyaloshinskii vector, we refer to the analytical solution given by Dzyaloshinskii in Ref. 27 and the detailed review in Ref. 34.

A. Conditions for a collinear domain magnetization

In this section, we present some analytical results concerning the transition between collinear and noncollinear domain magnetization. We start with the case that **D** points parallel to the easy axis. Then, we discuss the case that **D** is perpendicular to the easy axis.

1. *Dzyaloshinskii vector parallel to the easy axis*

If the Dzyaloshinskii vector points parallel to the easy axis, there is a continuous transition from a collinear to a noncollinear domain magnetization (cf. Fig. 3). In the following it is shown, that the corresponding critical line is given by Eq. (15).

In Cartesian coordinates $\{m_j\} = \{\hat{\mathbf{e}}_j \cdot \mathbf{m}\}$, the functional (10) reads

$$E_{\rm II} = \int \mathrm{d}x_{\rm II} \big[\dot{m}_1^2 + \dot{m}_2^2 + \dot{m}_3^2 + K_{\rm II}\, m_1^2 + m_2^2 + D_{\rm II}\,(m_1\,\dot{m}_2 - \dot{m}_1\,m_2) \big] \tag{23}$$

and the condition $m_1^2 + m_2^2 + m_3^2 = 1$ reduces the degrees of freedom. We want to discuss the magnetization in the vicinity of the collinear state with $\mathbf{m} = \hat{\mathbf{e}}_3 \,\|\, \mathbf{D}$. In this regime we can neglect $\dot{m}_3^2$ against $\dot{m}_1^2 + \dot{m}_2^2$, since m_3 is stationary at $\mathbf{m} = \hat{\mathbf{e}}_3$. With this approximation, we obtain the Euler-Lagrange equations

$$2\,K_{\rm II}\,m_1 + 2\,D_{\rm II}\,\dot{m}_2 - 2\,\ddot{m}_1 \;=\; 0\,, \tag{24}$$

$$2\,m_2 - 2\,D_{\rm II}\,\dot{m}_1 - 2\,\ddot{m}_2 \;=\; 0\,. \tag{25}$$

The existence of a noncollinear state that is restricted to $\mathbf{m} \approx \hat{\mathbf{e}}_3$ implies a non-trivial bounded solution of the Eqs. (24-25) (the trivial solution $m_1 \equiv m_2 \equiv 0$ corresponds to the collinear state). In the following we derive a criteria for the existence of bounded solutions. Using (24) to express $\dot{m}_2$ by m_1, $\ddot{m}_1$ and inserting this into the derivative of (25) leads to the 4th-order linear differential equation

$$K_{\rm II}\,m_1 + (D_{\rm II}^2 - 1 - K_{\rm II})\,\ddot{m}_1 + \ddot{\ddot{m}}_1 = 0\,. \tag{26}$$

The real and bounded solutions of (26) are restricted to linear combinations of $\{\cos(\omega\, x_{\rm II}),\, \sin(\omega\, x_{\rm II})\}_\omega$, where $\omega = -i\,\nu$ is given by the purely imaginary roots of the characteristic polynomial

$$P(\nu) = \nu^4 + (D_{\rm II}^2 - 1 - K_{\rm II})\,\nu^2 + K_{\rm II} = 0\,. \tag{27}$$

With the substitution $\mu = \nu^2$ we need to derive the conditions for negative real roots of the polynomial

$$P'(\mu) = \mu^2 + (D_{\rm II}^2 - 1 - K_{\rm II})\,\mu + K_{\rm II} = 0\,. \tag{28}$$

The last equation can be rewritten as

$$\big(2\,\mu + D_{\rm II}^2 - 1 - K_{\rm II}\big)^2 = (D_{\rm II}^2 - 1 - K_{\rm II})^2 - 4\,K_{\rm II}\,, \tag{29}$$

thus μ is real if and only if

$$(D_{\rm II}^2 - 1 - K_{\rm II})^2 > 4\,K_{\rm II} = (2\,\sqrt{K_{\rm II}}\,)^2 \;\;\Rightarrow \begin{cases} D_{\rm II}^2 > (1 + \sqrt{K_{\rm II}}\,)^2 & \text{if } D_{\rm II}^2 > 1 + K_{\rm II} \\ D_{\rm II}^2 < (1 - \sqrt{K_{\rm II}}\,)^2 & \text{if } D_{\rm II}^2 < 1 + K_{\rm II} \end{cases} \tag{30}$$

(in the last formulas we used that $K_{\rm II} > 0$ for **D** parallel to the easy axis, and we employed the relation $\pm 2\,\sqrt{K_{\rm II}} = (1 \pm \sqrt{K_{\rm II}}\,)^2 - 1 - K_{\rm II}$). The next step is to check the sign of μ. With $C = D_{\rm II}^2 - 1 - K_{\rm II}$, Eq. (28) yields

$$\begin{aligned} 2\,\mu \;&=\; -C \pm \sqrt{C^2 - 4\,K_{\rm II}} \\ &=\; -(\operatorname{sign} C)\,\sqrt{C^2} \pm \sqrt{C^2 - 4\,K_{\rm II}}\,, \end{aligned} \tag{31}$$

provided that μ is real. From the last equation it is obvious, that

$$\operatorname{sign}\mu = -\operatorname{sign}(D_{\rm II}^2 - 1 - K_{\rm II}) \quad \text{if } \mu \text{ real}\,. \tag{32}$$

Combining Eqs. (30) and (32), we conclude that the energy functional (10) is not minimized by a any noncollinear magnetization with $\mathbf{m} \approx \hat{\mathbf{e}}_3 \| \mathbf{D}$ if

$$|D_{\rm II}| < 1 + \sqrt{K_{\rm II}}\,, \tag{33}$$

thus we obtain Eq. (15). In order to confirm that our noncollinear solution indeed yields a lower energy than the trivial collinear solution, we have to insert a linear combination of $\{\cos(\sqrt{-\mu}\,x_{\rm II}),\, \sin(\sqrt{-\mu}\,x_{\rm II})\}_\mu$ (with $\{\mu\}$ given by Eq. (31)) in the energy functional. This lengthy calculation is omitted here, but numerical calculations show that the noncollinear state emerging at $|D_{\rm II}| > 1 + \sqrt{K_{\rm II}}$ is energetically favorable.

We note, that the Eqs. (24-25) determine the optimal ratio, but not the prefactor of $m_1(x)$ and $m_2(x)$. However, the numerical investigation (that does not neglect the term $\dot{m}_3^2$ in Eq. (23)) shows a continuous transition at $|D_{\rm II}| = 1 + \sqrt{K_{\rm II}}$.

A special situation arises if there is no anisotropy in the plane normal to the Dzyaloshinskii vector (i.e. $K_{\rm II} = 1$). In this case, the ground state undergoes a first-order transition from a collinear state to a flat rotating spiral when $|D_{\rm II}|$ increases (point c in Fig. 3a). As already mentioned in section III A, for $K_{\rm II} = 1$ the functional (10) reduces to (14) and the phase transition occurs at

$$\dot{\varphi}^2 + D_{\rm II}\,\dot{\varphi} + 1 = 0\,. \tag{34}$$

For $\dot{\varphi} = \text{const}$ the right-hand side of Eq. (34) is minimized by $\dot{\varphi} = -\frac{D_{\rm II}}{2}$. Inserting this in (34) yields

$$|D_{\rm II}| = 2\,. \tag{35}$$

Of course, this result is just a special case of the condition (33).

2. Dzyaloshinskii vector perpendicular to the easy axis

If the Dzyaloshinskii vector is in a plane perpendicular to the easy axis, a pointwise continuous transition from the collinear to a noncollinear state is not possible. This is plausible, since the noncollinear state gains energy only from a rotation around the Dzyaloshinskii vector. For more rigorous argumentation, we use the same procedure as above. If the easy axis is parallel to $\hat{\mathbf{e}}_1$, we can express m_1, $\dot{m}_1$ by m_2, m_3, $\dot{m}_2$, $\dot{m}_3$ in Eq. (23), expand the integrand around $m_2 = m_3 = \dot{m}_2 = \dot{m}_3 = 0$ and neglect all but the leading terms. Then we obtain the integrand

$$\dot{m}_2^2 + \dot{m}_3^2 + K_{\mathrm{II}}\,(1 - m_2^2 - m_3^2) + m_2^2 + D_{\mathrm{II}}\,\dot{m}_2$$

and the corresponding Euler-Lagrange equations

$$2\,(1 - K_{\mathrm{II}})\,m_2 - 2\,\ddot{m}_2 \;=\; 0\,, \tag{36}$$

$$-\,2\,K_{\mathrm{II}}\,m_3 - 2\,\ddot{m}_3 \;=\; 0\,. \tag{37}$$

These equations have no bounded solution for any $K_{\mathrm{II}} < 0$, i.e. for $K_1 < K_D < K_2$. Thus, if $\mathbf{D}$ points parallel to the intermediate axis there is no stable noncollinear solution in the vicinity of the collinear solution. If $\mathbf{D}$ points parallel to the hard axis, we cannot use the ansatz (23) since the transformation (8) is not defined in this case. But, in this case we can work with the simplified functional (12). It is obvious, that this functional is not minimized by any function with non-constant $\operatorname{sign}\dot{\varphi}$: The term $(\dot{\varphi}^2 + \sin^2\varphi)$ gives a positive contribution to the energy for all $\varphi \not\equiv 0$, whereas the integral

$$\int \mathrm{d}x_{\mathrm{I}}\, D_{\mathrm{I}}\,\dot{\varphi} \;=\; \int\limits_{\{\varphi|\dot{\varphi}>0\}} \mathrm{d}\varphi\, D_{\mathrm{I}} \;-\; \int\limits_{\{\varphi|\dot{\varphi}<0\}} \mathrm{d}\varphi\, D_{\mathrm{I}} \tag{38}$$

vanishes over one spatial period if the magnetization does not perform a full rotation around the $\mathbf{D}$-vector.

The critical line, that separates the regions labeled (Col $\perp$ $\mathbf{D}$) and (NC $\perp$ $\mathbf{D}$) in Fig. 3, also corresponds to a second-order phase transition from a collinear to a flat rotating magnetic structure. However, at this transition the magnetization is not pointwise continuous. If $|D|$ is approaching the transition point from above, the magnetization shows a periodic structure of almost collinear domains and the period length diverges at the transition point. At this transition, the magnetization is confined to the plane normal to the Dzyaloshinskii vector. This case is discussed analytically in Refs. 27,34.

B. Domain walls

If the magnetization is confined to a plane, the integration over the DM term is straightforward (cf. Eq. (19)) and we can employ the analytical solution that is given by Landau and Lifshitz in Ref. 2.

A further simple analytic solution exists in the case that the Dzyaloshinskii vector points parallel to the easy axis and there is no anisotropy in the plane normal to $\mathbf{D}$ (i.e. $K_{\mathrm{II}} = 1$ or $K_D < K_1 = K_2$). In this case the system can be described with the energy functional (14). Obviously, this functional is not minimized if the φ-dependent factor $(\dot{\varphi}^2 + D_{\mathrm{II}}\,\dot{\varphi} + 1)$ is not minimized for all x. Thus, we obtain

$$\dot{\varphi}\big|_{\mathrm{K_{II}}=1} = -\,\frac{D_{\mathrm{II}}}{2} \tag{39}$$

(cf. Eq. (34)) and Eq. (14) simplifies to

$$E_{\mathrm{II}}\Big|_{K_{\mathrm{II}}=1} = \int \mathrm{d}x_{\mathrm{II}} \left[\dot{\vartheta}^2 + \sin^2\vartheta\left(1 - \frac{D_{\mathrm{II}}^2}{4}\right)\right]. \tag{40}$$

This equation is equivalent to Eq. (12) with an effective anisotropy parameter $(1 - \frac{1}{4}\,D_{\mathrm{II}}^2)$. If this parameter is positive, we can employ the solution of Eq. (17) and obtain

$$\vartheta = \pm \arccos\tanh\left(-\sqrt{1 - \frac{D_{\mathrm{II}}^2}{4}}\,x_{\mathrm{II}}\right) \tag{41}$$

and

$$E_{\mathrm{II}} = 4\sqrt{1 - \frac{D_{\mathrm{II}}^2}{4}}\,. \tag{42}$$

The case $1 - \frac{1}{4}\,D_{\mathrm{II}}^2 < 0$ implies that the magnetic structure is confined to the plane normal to the easy axis (cf. Eqs. (34) and (35)). In this case, our model does not show different domains and hence does not show domain walls.

If we introduce an anisotropy in the plane normal to the Dzyaloshinskii vector (i.e. $K_{\mathrm{II}} \neq 1$), $\dot{\varphi}$ is not constant as the magnetization tries to avoid the hard axis (cf. inset of Fig. 6). But if $\mathbf{D}$ points parallel to the easy axis, the wall magnetization cannot be confined to the plane normal to the hard axis. This can be seen from the Euler-Lagrange equation of the functional (10):

$$\begin{aligned} 0 = \;& 2\,(D_{\mathrm{II}} + 2\,\dot{\varphi})\,\dot{\vartheta}\,\sin\vartheta\,\cos\vartheta + 2\,\ddot{\varphi}\,\sin^2\vartheta \\ & -\,2\,(K_{\mathrm{II}} - \sin^2\vartheta)\,\sin\varphi\cos\varphi\;. \end{aligned} \tag{43}$$

For $\varphi = 0 = \mathrm{const}$ (if $0 < K_{\mathrm{II}} < 1$) or $\varphi = \pi/2 = \mathrm{const}$ (if $1 < K_{\mathrm{II}}$) the Eq. (43) simplifies to

$$0 = D_{\mathrm{II}}\,\dot{\vartheta}\,\sin\vartheta\,\cos\vartheta\,, \tag{44}$$

this equation cannot be fulfilled for $D_{\mathrm{II}} \neq 0$ and $\vartheta \neq \mathrm{const}$.

V. SUMMARY

The inclusion of the Dzyaloshinskii-Moriya interaction in a simple micromagnetic model can lead to a variety of possible magnetic phases at zero temperature. Depending on the on the anisotropy constants and the size and

orientation of the Dzyaloshinskii vector, the domain magnetization can be collinear, spatially rotating within one plane or truly three-dimensional. The latter case requires an anisotropy in the plane normal to the Dzyaloshinskii vector.

Even in the regime of collinear magnetized domains, the domain-wall magnetization can be confined to a plane or perform a three-dimensional path in spin space. If the Dzyaloshinskii vector points parallel to the easy axis, the wall magnetization can perform an infinite number of rotations.

VI. ACKNOWLEDGMENTS

We thank C. Friedrich and R. Hertel for valuable suggestions during the course of this work. We acknowledge financial support from the Deutsche Forschungsgemeinschaft (Grant no. BI823/1-1) and from the ESF EUROCORES Programme SONS (Contract no. ERAS-CT-2003-980409).

[1] F. Bloch, Z. Phys. **74**, 295 (1932).
[2] L. Landau and E. Lifshitz, Phys. Z. Sowjetunion **8**, 153 (1935).
[3] L. Néel, C. R. Acad. Sci. (Paris) **241**, 533 (1955).
[4] A. Hubert and R. Schäfer, *Magnetic Domains* (Springer-Verlag, Berlin, 1998).
[5] S. Datta and B. Das, Appl. Phys. Lett. **56**, 665 (1990).
[6] J. Grollier, D. Lacour, V. Cros, A. Hamzic, A. Vaurès, A. Fert, D. Adam, and G. Faini, J. Appl. Phys. **92**, 4825 (2002).
[7] I. Žutić, J. Fabian, and S. Das Sarma, Rev. Mod. Phys. **76**, 323 (2004).
[8] D. A. Allwood, G. Xiong, C. C. Faulkner, D. Atkinson, D. Petit, and R. P. Cowburn, Science **309**, 1688 (2005).
[9] S. S. P. Parkin, M. Hayashi, and L. Thomas, Science **320**, 190 (2008).
[10] M. Bode, Rep. Prog. Phys. **66**, 523 (2003).
[11] A. Yamaguchi, T. Ono, S. Nasu, K. Miyake, and T. Shinjo, Phys. Rev. Lett. **92**, 077205 (2004).
[12] S. Meckler, N. Mikuszeit, A. Preßler, E. Y. Vedmedenko, O. Pietzsch, and R. Wiesendanger, Phys. Rev. Lett. **103**, 157201 (2009).
[13] R. Wiesendanger, Rev. Mod. Phys. **81**, 1495 (2009).
[14] A. J. Freeman and C. L. Fu, J. Appl. Phys. **61**, 3356 (1987).
[15] R. Skomski, J. Phys.: Condens. Matter **15**, R841 (2003).
[16] P. Ferriani, , S. Heinze, G. Bihlmayer, and S. Blügel, Phys. Rev. B **72**, 024452 (2005).
[17] Y. Mokrousov, A. Thiess, and S. Heinze, Phys. Rev. B **80**, 195420 (1909).
[18] I. E. Dzialoshinskii, Sov. Phys. JETP **5**, 1259 (1957).
[19] T. Moriya, Phys. Rev. **120**, 91 (1960).
[20] A. Fert, Materials Science Forum **59-60**, 439 (1990).
[21] M. Bode, M. Heide, K. von Bergmann, P. Ferriani, S. Heinze, G. Bihlmayer, A. Kubetzka, O. Pietzsch, S. Blügel, and R. Wiesendanger, Nature (London) **447**, 190 (2007).
[22] P. Ferriani, K. von Bergmann, E. Y. Vedmedenko, S. Heinze, M. Bode, M. Heide, G. Bihlmayer, S. Blügel, and R. Wiesendanger, Phys. Rev. Lett. **101**, 027201 (2008).
[23] R. Mazzarello and E. Tosatti, Phys. Rev. B **79**, 134402 (2009).
[24] A. N. Rudenko, V. V. Mazurenko, V. I. Anisimov, and A. I. Lichtenstein, Phys. Rev. B **79**, 144418 (2009).
[25] S. Mankovsky, S. Bornemann, J. Minár, S. Polesya, H. Ebert, J. B. Staunton, and A. I. Lichtenstein, Phys. Rev. B **80**, 014422 (2009).
[26] M. Heide, G. Bihlmayer, and S. Blügel, Phys. Rev. B **78**, 140403(R) (2008).
[27] I. E. Dzyaloshinskiĭ, Sov. Phys. JETP **20**, 665 (1965).
[28] U. K. Rößler, A. N. Bogdanov, and C. Pfleiderer, Nature (London) **442**, 797 (2006).
[29] A. Bogdanov and A. Hubert, J. Magn. Magn. Mater. **138**, 255 (1994).
[30] B. Binz and A. Vishwanath, Phys. Rev. B **74**, 214408 (2006).
[31] S. Mühlbauer, B. Binz, F. Jonietz, C. Pfleiderer, A. Rosch, A. Neubauer, R. Georgii, and P. Böni, Science **323**, 915 (2009).
[32] A. B. Butenko, A. A. Leonov, A. N. Bogdanov, and U. K. Rößler, Phys. Rev. B **80**, 134410 (2009).
[33] H. J. G. Draaisma and W. J. M. de Jonge, J. Appl. Phys. **64**, 3610 (1988).
[34] Y. A. Izyumov, Sov. Phys. Usp. **27**, 845 (1984).
[35] M. Heide, Ph.D. thesis, RWTH Aachen (2006).